Structure and arrangement of clusters in cluster aggregation

M. D. Haw, W. C. K. Poon, and P. N. Pusey
Department of Physics and Astronomy, The University of Edinburgh, King's Buildings, Mayfield Road, Edinburgh, EH9 3JZ, United Kingdom
(Received 26 February 1997)

We study cluster structure and the arrangement of clusters in the diffusion-limited cluster-cluster aggregation (DLCA) simulation model of colloidal aggregation, analyzing our data using techniques that allow direct comparison with scattering experiments. As is well known, individual clusters in DLCA have a fractal structure; we compare DLCA results with colloidal aggregation experiments by fitting the Fisher-Burford [Phys. Rev. **156**, 583 (1967)] functional form for the scattering by a fractal object to the average scattering function or form factor of DLCA clusters. In two-dimensional (2D) simulations the DLCA average form factor deviates from the Fisher-Burford form, though power-law fits to the data do give fractal dimensions in agreement with the ''accepted'' fractal dimension of 2D DLCA clusters previously obtained from the fractal mass-radius relation. The average form factor in 3D simulations agrees better with the Fisher-Burford form though there remain indications of some deviation. Near gelation, the average form factor at long length scales begins to *decrease*, corresponding to the interpenetration and assembly of the clusters into the system-spanning gel. We also study the arrangement of clusters or the intercluster structure by computing the cluster center-of-mass structure factor. The cluster structure factor demonstrates a strong ''excluded-volume'' interaction between the clusters. As the aggregation proceeds, while larger clusters are distributed more or less evenly, there is a marked inhomogeneity in the distribution of the *smallest* clusters, especially pronounced at high particle concentration. The *polydispersity* of the clusters thus has important effects on the cluster arrangement. We find that the total scattering function *cannot* be factorized into the average form factor and the cluster center-of-mass structure factor, due at least in part to the size-position correlation thus induced by the cluster polydispersity. We also examine the ''mass-weighted'' cluster structure factor as considered previously by other authors [F. Sciortino, A. Belloni, and P. Tartaglia, Phys. Rev. E **52**, 4068 (1995)]. [S1063-651X(97)06608-7]

PACS number(s): 61.43.Hv, 82.70.−y

I. INTRODUCTION

Recent experiments have demonstrated some surprising aspects of the structure of aggregating colloidal suspensions [1–9]. While early experiments and computer simulations [10–12] concentrated on the fractal structure of *individual* clusters of colloidal particles, small-angle light-scattering experiments have demonstrated that the intercluster structure of the system is far from trivial. A growing characteristic length scale is indicated by the presence of a strong peak in the scattered intensity at small angles. The peak moves to smaller angle and grows brighter as the aggregation proceeds. Very similar results have been obtained from the most recent computer simulations using the diffusion-limited cluster aggregation (DLCA) model [13–19]. Similar results are also seen in other experimental systems, for instance, the system of siloxane polymers studied by Cabane and coworkers [20–22]. However, a complete understanding of the scattering behavior of the aggregating system in terms of definable physical elements of structure has yet to be achieved. In this paper we study the scattering behavior of the DLCA system in more detail than previous analyzes, to investigate both the structure of individual clusters and the cluster *arrangement* or intercluster structure.

The paper is ordered as follows. In the next section we describe briefly the simulation model and the basic methods of the ''scattering'' analysis of the simulation results. Thereafter we discuss separately the analysis of cluster structure and cluster arrangement in the DLCA system. Finally, we briefly consider the factorization of the ''total'' scattering function of the aggregating system into functions describing the cluster structure and the cluster arrangement, discussing at the same time similar approaches by other authors [7,23].

II. METHODS

The DLCA model of aggregating colloidal suspensions has been the subject of many studies since its introduction by Meakin [10] and by Kolb *et al.* [11]. We have described our own (standard) implementation of the model in detail elsewhere [17] and give only brief details here. N colloidal ''particles'' are placed at random onto an $L\times L$ [in two dimensions (2D)] or $L\times L\times L$ (in 3D) lattice. Periodic boundary conditions are implemented. Before initiation of aggregation the particle starting coordinates are further randomized in order that we begin with a ''fluidlike'' structure. Thence the particles diffuse by carrying out a random walk on the lattice. Particles that become nearest neighbors are joined so that they belong to the same cluster; thereafter the cluster diffuses as a whole and may collide and join with other clusters or particles. We scale the diffusion coefficient of a cluster in inverse proportion to its radius of gyration:

$$D\sim R_g^{-1}, \tag{1}$$

in order to simulate the physical slowing of the diffusion of larger clusters. (Note that such a scaling of cluster diffusion

rate, while not always implemented (e.g., [15]), has important consequences for the kinetics of the aggregation [17,24].)

In the simulations analyzed here, we have used lattices of $L=300$ or $L=500$ in 2D and $L=70$ in 3D. Further, we have studied a small range of number densities ρ ($\rho=0.01$, 0.1, and 0.3 in 2D and $\rho=0.01$, 0.05, and 0.1 in 3D). Since $N=\rho L^D$, where $D=2$ or 3, we have typically $N=2500$ ($\rho=0.01$ in 2D) to $N=75\,000$ ($\rho=0.3$, $L=500$ in 2D).

The scattering function of a system of N particles $I(\mathbf{Q})$ is given by

$$I(\mathbf{Q})=\frac{1}{N}\sum_{j}^{N}\sum_{k}^{N}\exp[i\mathbf{Q}\cdot(\mathbf{r}_j-\mathbf{r}_k)], \tag{2}$$

where $\mathbf{Q}$ is the scattering vector and $\mathbf{r}_j$ and $\mathbf{r}_k$ are the particle coordinates. The above function is sometimes referred to as the *structure factor*; see e.g., [13,16–19]. For clarity, since below we discuss the *cluster center-of-mass* structure factor that describes the arrangement of clusters, in this paper we shall call $I(Q)$ the *total scattering function*. Note that in an experiment the intensity (of light, x rays, neutrons, etc.) scattered by the system involves a multiplicative factor describing the scattering by an individual particle (the single-particle form factor); in the simulations we take this as a constant, independent of $\mathbf{Q}$, and thus for simplicity leave it out of our expressions. This is equivalent to treating the simulation particles as ''δ functions'' or point masses.

For a simulation box of side L the scattering vectors allowed by the periodic boundary conditions in each dimension are given by $Q=\pm 2n\pi/L$, where n is an integer. Therefore, the reciprocal space represented by the set of allowed scattering vectors consists of a square (in 2D) or cubic (in 3D) lattice of points, with lattice spacing $2\pi/L$. For these lattice-based simulations, the total scattering functions, cluster form factors, and inter-cluster structure factors (see below) may be evaluated using the discrete fast Fourier transform algorithm [25]. The calculated scattering functions are circularly or spherically averaged in thin annuli of width δQ (typically $\delta Q=0.1$ reciprocal particle diameters) and plotted against scattering vector magnitude Q.

The evolution of the total scattering function of the DLCA system has been examined and compared with colloidal light scattering experiments by a number of authors [13,16–19]. Briefly, the DLCA simulation displays features in qualitative agreement with experiment: $I(Q)$ develops a peak at small but nonzero Q and this peak grows in intensity and moves to smaller Q as the aggregation proceeds and larger and larger fractal clusters of particles are formed. At late time *gelation* may occur: In any system at finite particle concentration with irreversible particle ''bonding,'' the growth of the fractal clusters results eventually in the filling of space and the formation of a system-spanning macroscopic ''gel'' cluster (see, e.g., [9]). In the simplest model the gel is an assembly of fractal clusters whose size R_{gel} is system number-density dependent; thus, in a simulation system not substantially bigger than R_{gel} the gel structure cannot be correctly formed and at the final stage the system contains instead a single isolated fractal cluster. In the case of our simulations, this means that we are able to examine the effects of gelation only in systems at high enough number density.

III. CLUSTER STRUCTURE

At any given time t the simulation system contains a number of clusters of different masses. The intensity scattered by a given *isolated* cluster of particles (which we label cluster k), the *single cluster form factor* $P_k(\mathbf{Q})$, is obtained by inserting the set of coordinates of the particles belonging to cluster k into Eq. (2):

$$P_k(\mathbf{Q})=\frac{1}{M_k}\sum_{j}^{M_k}\sum_{l}^{M_k}\exp[i\mathbf{Q}\cdot(\mathbf{r}_j-\mathbf{r}_l)]. \tag{3}$$

M_k is the total number of particles in the cluster (the cluster mass). We compute the *average* cluster form factor $P(\mathbf{Q},t)$ over the ensemble of clusters in the system from

$$P(\mathbf{Q},t)=\frac{1}{\sum_{k}^{N_c}M_k}\sum_{k}^{N_c}M_kP_k(\mathbf{Q}), \tag{4}$$

where the average is taken over the $N_c(t)$ clusters in the system and each individual cluster's ''normalized'' form factor $P_k(\mathbf{Q})$ [Eq. (3)] is *weighted by the mass of the cluster* M_k. This form of average is equivalent to the scattering that would be seen from a dilute (polydisperse) system of clusters in an experiment: Larger clusters scatter more. The analogous experiment is to measure the scattering by a system that is *diluted* (and the aggregation effectively stopped) at time t, assuming that the dilution process does not affect the structure of the clusters themselves. This experimental procedure has been used to study the onset of gelation in polymer systems [26] and a few similar experiments have been attempted in systems more akin to colloids [20–22,27], as is discussed below.

A. Form factor of a fractal cluster

It has been amply demonstrated that the clusters of particles in DLCA have a fractal structure [10,11]. Simple limiting forms are expected for the scattering function of a single circularly or spherically symmetric fractal object (see, e.g., [28]):

$$P(Q)\sim Q^{-d_f}\quad (Q_l<Q\ll Q_u), \tag{5}$$

$$P(Q)\to M\quad (Q\to 0), \tag{6}$$

where M is the cluster mass, d_f is the fractal dimension of the cluster, and Q_l and Q_u are the lower and upper reciprocal space cutoffs, respectively; $2\pi/Q_l$ corresponds to a length scale of the size of the cluster and $2\pi/Q_u$ approximately to the size of the ''monomers'' making up the cluster. A more detailed functional form that has been used to fit experimental light-scattering data for aggregating colloidal systems [27], essentially a combination of the limiting forms in Eqs. (5) and (6), is given by the Fisher-Burford (FB) expression (see, e.g., [22,29])

$$P(Q)=\frac{A}{[1+2Q^2R_g^2/3d_f]^{d_f/2}}. \quad (7)$$

R_g is a measure of the cluster radius, d_f is the fractal dimension, and A is proportional to the cluster mass [7]. This function includes both the power-law region $P(Q)\sim Q^{-d_f}$ at larger Q and the ''rollover'' to the Guinier regime as Q approaches zero:

$$P(Q\rightarrow 0)\rightarrow A\left(1-\frac{Q^2R_g^2}{3}\right). \quad (8)$$

Plotting P vs QR_g demonstrates that the rollover corresponds approximately to $QR_g=1$ or $Q_l\approx 2\pi/R_g$.

''Accepted'' estimates of the DLCA cluster fractal dimension have been obtained from plots of cluster mass versus cluster radius in large-scale simulations [10–12], giving $d_f\approx 1.4$ in 2D and $d_f\approx 1.75$ in 3D. An estimation of the power-law exponent from the power-law region in $P(Q)$ is sometimes used to obtain the fractal dimension of the clusters [30]. It should be remembered that the estimation of fractal dimension from the average form factor involves averaging over clusters whose structures may vary. This also applies to estimates of d_f from mass-radius plots (e.g., [31,32]) and of course to most experimental measures of the fractal dimension of real systems, whether obtained by imaging or scattering methods.

B. Results

Plots of the calculated average form factors $P(Q,t)$ for various times t in simulations at various number densities ρ, in 2D and 3D, are given in Fig. 1. P is plotted against Qd, where d is the particle diameter (in these cases d is equal to one lattice spacing, of course). Since monomers are treated as δ functions in the scattering equations, for an initial system consisting only of monomers we would have $P(Q,t=0)=1.0$. In fact, on the lattice there are always some small clusters of particles even at time $t=0$ [17]. As the aggregation proceeds the scattering by the ''average cluster'' increases at small Q, indicating the growth of larger and larger structures. For $Q>Q_l$ the scattering function is expected to follow a power law in Q as in Eq. (5). In fact, on the log-log plots it is clear that through early times the average form factor does not show a constant power-law exponent. At such early times the system includes a range of small clusters that show little fractal structure.

We consider in detail the results from the two-dimensional simulations first. In Fig. 2 we show an attempt to fit the Fisher-Burford function (7) to the $P(Q)$ data from a two-dimensional simulation at number density $\rho=0.01$. It is clear that the fit is not very good at large Q and becomes progressively worse at later times. Results from simulations at higher number densities are similar. The two-dimensional $P(Q)$ curve seems to consist of three regions. At large Q we find a power-law region that extends to smaller and smaller Q at later times as the clusters grow larger. At small Q we see the near-flat rollover region in $P(Q)$. However, between these regions there is a third, with a *steeper* slope on the log-log plots than the power-law region at large Q. The Fisher-Burford function is not adequate to fit a curve of this form. In practice the fit fails at large Q and the ''fractal dimension'' parameter in Eq. (7), fitted to the steeper slope of the middle region of the $P(Q)$ curve, is certainly not a good estimate of the fractal dimension of the clusters.

The reasons for the shape of the $P(Q)$ curve from the two-dimensional simulations are not clear. Conceivably the marked anisotropy of the clusters (and possibly even an orientational correlation between neighboring clusters) might have significant effects on the average form factor, especially at later times when there are fewer clusters in the system. The polydispersity of the clusters may also have effects that are not ''washed out'' in the averaging over the ensemble of clusters. Alternatively the deviation from the Fisher-Burford form may be some effect of the underlying lattice. However, calculations using data from an *off-lattice* simulation in 2D [13] show a very similar form for the average cluster form factor. It is interesting to notice that fitting a simple power law, as in Eq. (5), to the power-law region of $P(Q)$ at large Q (where that region extends over a reasonable range of Q) gives estimates of the cluster fractal dimension in good agreement with the ''accepted'' estimate for two-dimensional DLCA [12], $d_f\approx 1.4$ (Table I). To verify whether the effects we observe in our simulated $P(Q)$ may yet be artifacts of the simulation model, experiments that directly measure $P(Q)$ [i.e., $P(Q)$ and not simply the total scattering function $I(Q)$] would be of great value. We discuss possible experiments further in Sec. III C.

Next we consider the results from three-dimensional simulations. Fisher-Burford fits to the three-dimensional average form factor data seem more satisfactory than the two dimensional results; data and fits are shown in Fig. 3. However, the fractal dimension parameters obtained from these fits, as given in Table II, show a tendency to increase over time and to reach values higher than the accepted DLCA fractal dimension ($d_f\approx 1.75$ [12]) at late time, similar to the results from the two-dimensional simulations. For the latest times in the simulations at $\rho=0.05$ and $\rho=0.1$, where the rollover region in $P(Q)$ is no longer visible, we have also fitted a power-law relation to the $P(Q)$ data (Table II); we find again that typically the dimension estimated from the power law is lower than that from the Fisher-Burford fit and that the power-law estimates are in better agreement with the accepted fractal dimension.

An average fractal dimension d_f for the DLCA simulations may also be estimated from the form factor data by plotting the Fisher-Burford fit parameters A vs R_g. A is proportional to $P(Q\rightarrow 0)$ [Eq. (8)], which in turn is proportional to the weight average of the mass distribution; R_g is proportional to some characteristic radius of the clusters. Thus these parameters should be related according to the fractal mass-radius relation

$$A\sim R_g^{d_f}. \quad (9)$$

The plot is shown in Fig. 4, with estimates of d_f given in Table III. A power-law relation is observed over a good range in both R_g and A. For the lowest density where the clusters are smaller (at the times used for the fits), the estimate of d_f is slightly higher, possibly reflecting the fact that the underlying lattice structure affects the structure of smaller clusters more strongly. [The fractal dimension as es-

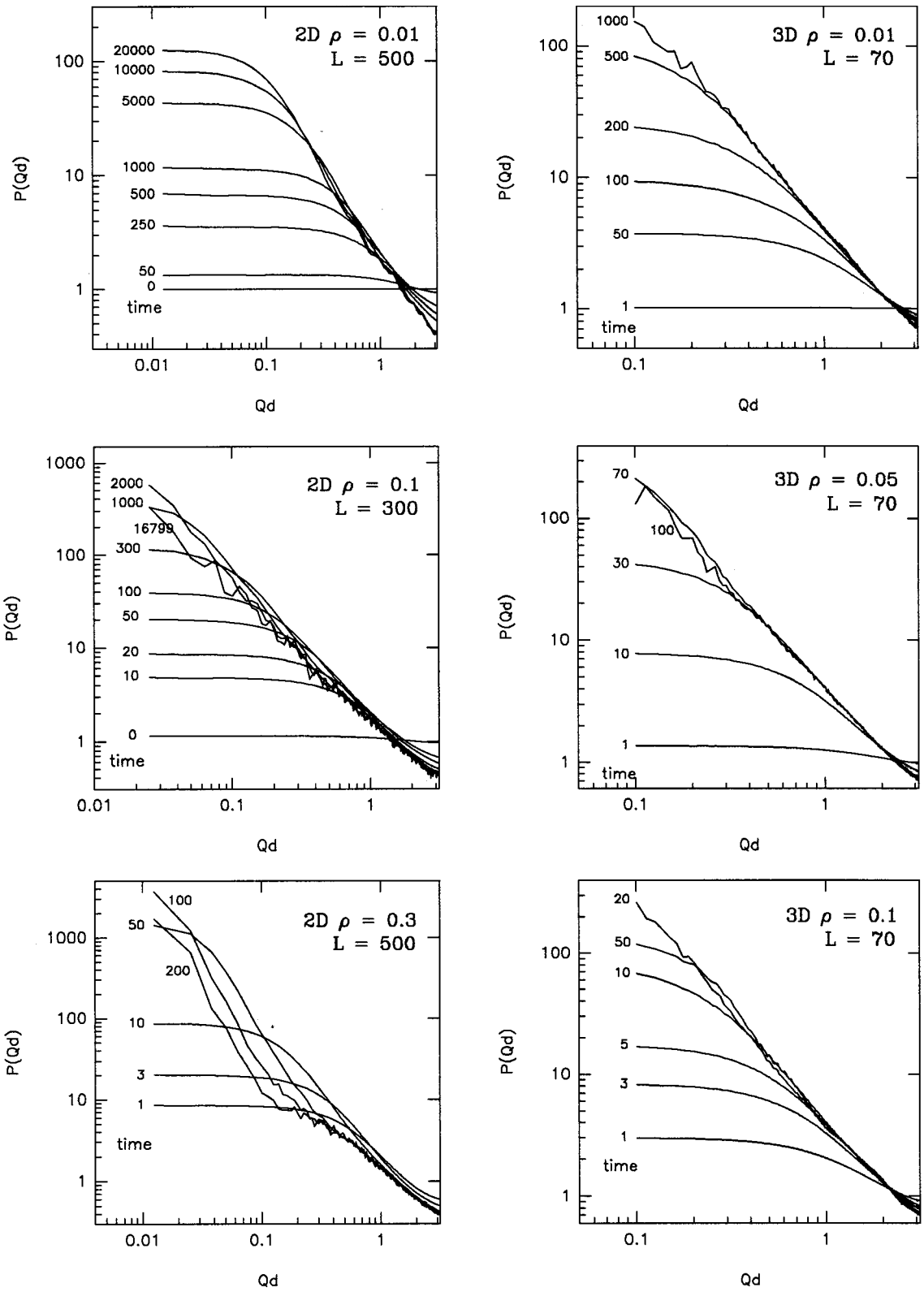

FIG. 1. Circularly or spherically averaged average form factors $P(Q,t)$ [in units as defined by Eq. (4)] for DLCA simulations in 2D (left column) and 3D (right column). ρ is the number density of the system and L is the system size in particle diameters; times t are indicated near each curve. The (dimensionless) x axis is Qd, where Q is the scattering vector magnitude in reciprocal particle diameters and d is the particle diameter.

timated from the total scattering function $I(Q)$ may also be somewhat dependent on system density, as demonstrated by results obtained for off-lattice simulations by Hasmy and Jullien [18].] However, the two higher densities and a fit including data from all densities give estimates of d_f in good agreement with the accepted fractal dimension of three-dimensional DLCA clusters.

The above Fisher-Burford analysis may be compared with

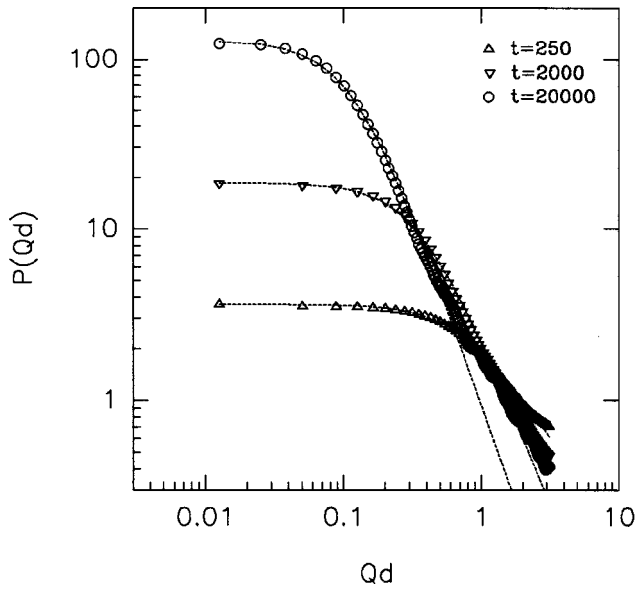

FIG. 2. Attempted fit of the Fisher-Burford function (7) to average cluster form factors $P(Q,t)$ from a two-dimensional simulation at number density $\rho=0.01$. Three example times t are shown. Units are as in Fig. 1.

experimental measurements in Ref. [27]. In that study Carpineti *et al.* fitted the Fisher-Burford form to scattering data from a low-concentration system of aggregating charged colloids. However, it is important to note that the measurements were of the total scattered intensity, *not* the average cluster form factor [i.e., $I(Q)$ as defined in Eq. (2), not $P(Q)$ from Eq. (4)]. While it might be expected that at low concentration correlations between clusters should be minimal, still of course in later work it was found that the scattered intensity showed a *peak* at nonzero Q even at small concentrations [1]. Regardless, in Ref. [27] good agreement of the scattered intensity with the Fisher-Burford form was found. The fractal dimension of the clusters was furthermore found to decrease with increasing concentration, possibly indicating, as Carpineti *et al.* point out, that the system investigated might not correspond to the ''ideal'' case of DLCA. On the other hand, as already mentioned, there are some indications from DLCA simulations too that d_f [as measured from $I(Q)$] is system density dependent and decreases with increasing concentration [17–19].

TABLE I. Power-law fits to the average form factor from two-dimensional simulations. The ''accepted'' 2D DLCA fractal dimension from mass-radius plots is $d_f \approx 1.4$ [10–12]. The ''averages'' give the ''typical'' dimension d_f with an error bar estimated from the variation over the different times. At density $\rho=0.3$ there appears to be so much change in the form of $P(Q)$ over time (see Fig. 1) that it is not reasonable to measure an average.

Density	Time	Qd range	d_f
0.01	2000	0.3–2.0	1.41
	5000	0.3–2.0	1.47
	10000	0.3–2.0	1.42
	20000	0.3–2.0	1.37
	average: 1.42 ± 0.05		
0.1	100	0.2–2.0	1.45
	300	0.3–2.0	1.43
	1000	0.2–2.0	1.38
	2000	0.2–2.0	1.39
	average: 1.42 ± 0.04		
0.3	10	0.3–2.0	1.58
	20	0.4–2.0	1.40
	30	0.4–2.0	1.28

C. Effect of gelation on $P(Q)$

As a consequence of the space-filling growth of fractal clusters, at the final stage of irreversible aggregation the system is filled by a single, spanning *gel* [9,17,18,31]. It is well known that the scattering function $I(Q)$ at this final stage retains a peak at nonzero Q (see, e.g., [9]). In the DLCA model, the gel is usually pictured as a near-homogeneous or possibly percolated [33] assembly of fractal clusters; the size of the fractal units in the assembly is strongly dependent on the overall system density and is related to the position of the peak in the scattered intensity [9].

When there is a single gel cluster left to which all the particles in the system belong, $P(Q)$ must trivially be equal to $I(Q)$ [Eqs. (2) and (3)]. Therefore, close to gelation, the magnitude of $P(Q)$ at small Q must drop substantially (over orders of magnitude) as $P(Q)$ changes from the fractal form [Eqs. (5) and (6)] to a function *peaked* at $Q>0$. As gelation is approached, ''fragments'' of the gel that are not fractal at the largest length scales are beginning to assemble and come to dominate the average form factor. We can observe these changes in $P(Q)$ from the DLCA simulations, especially in the highest number density systems. (As discussed previously, lower-density systems need to be much larger to properly obtain the long-length-scale structure of the gel, since in the gel assembly the size R_{gel} of the fractal units increases strongly with decreasing system density [9].) As shown in Fig. 5, in the two-dimensional, $\rho=0.3$ system, over times $t=100$ [$P(Q\rightarrow 0)\approx 3000$], $t=200$ [$P(Q\rightarrow 0)\approx 2000$], and $t=400$ [$P(Q\rightarrow 0)\equiv I(Q\rightarrow 0)\approx 3$, the final gel] the long-length-scale limit of $P(Q)$ falls by three orders of magnitude. Presumably this effect would be observable in an experiment in which the average form factor was measured by dilution of the system at times closer and closer to gelation. (In fact, just this procedure may be used to study gelation in *polymer* systems where bonds are chemical and dilution does not break up the clusters [26].) In the charged polystyrene colloid system studied by Carpineti *et al.* dilution was observed to have substantial effects on cluster structure [27]. However, interesting results have been obtained for a system in some ways intermediate between the typical colloidal system and the chemically bonded polymer system, that is, the siloxane system studied by Cabane and co-workers [20–22]. In these studies gelation is slow enough that good ''time resolution'' close to gelation can be obtained. Dubois and Cabane study the effect of increasing dilution on a sample extracted from the main reaction bath [21], showing that at large dilution, where the average form factor is measured equivalently to our calculations from the simulations, the small-Q peak in the scattering disappears and an FB-like form is obtained. As the authors point out, this demonstrates that the small-Q peak observed in the scattering function is

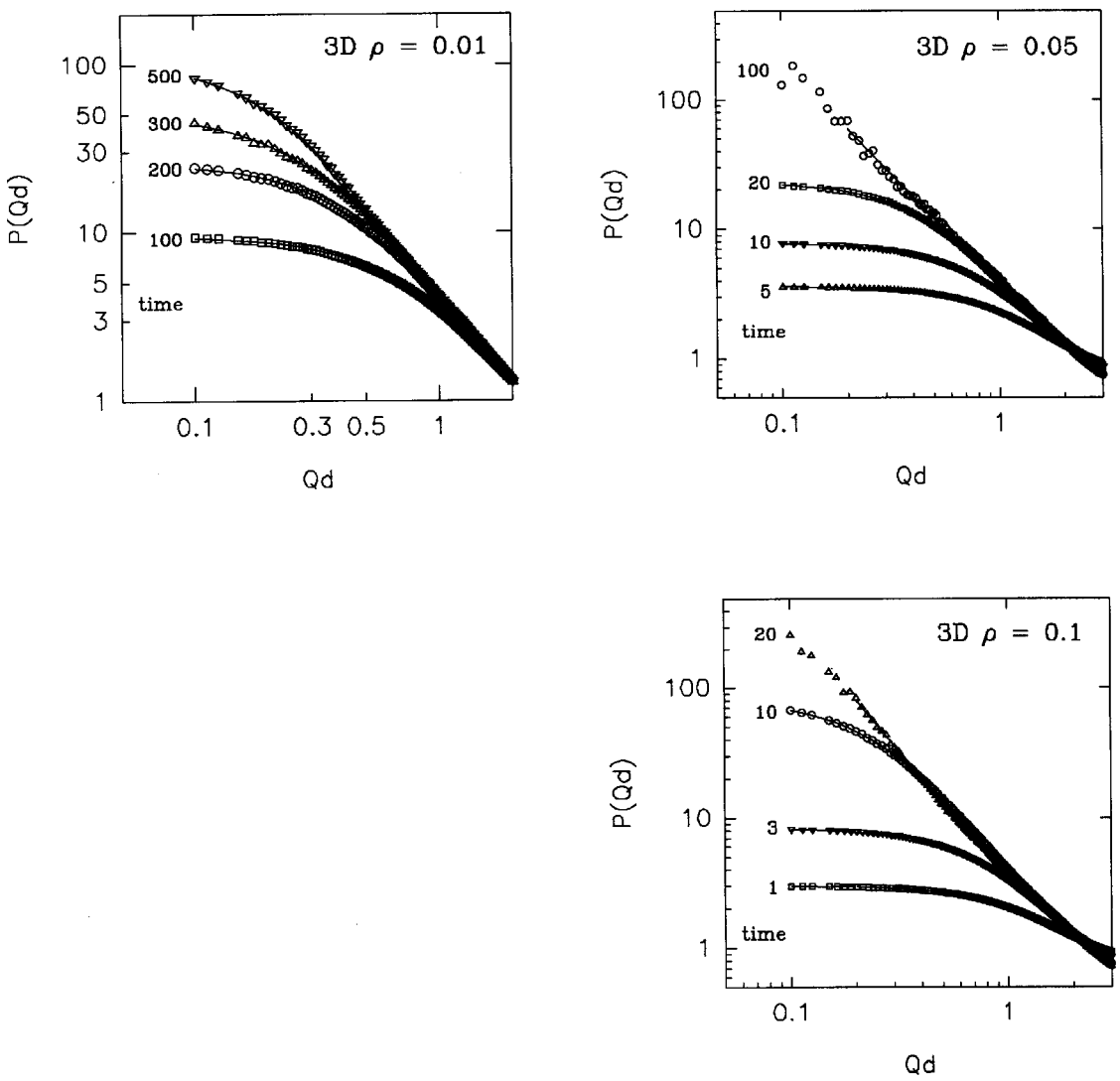

FIG. 3. Fits of the Fisher-Burford function (7) to average form factors $P(Q,t)$ for simulations in 3D. Units are as in Fig. 1. ρ is the number density of the system. The lines drawn are the best fits estimated by least squares; fit parameters are given in Table II. For $t=100$, $\rho=0.05$, and $t=20$, $\rho=0.1$, the lines are simple power laws rather than the Fisher-Burford expression; see also Table II.

due to *intercluster* interference. In fact, this work predates the more recent small-angle light scattering studies of, albeit in some ways simpler, colloidal systems [1–6,8]. However, the measured form factors do not seem to have been analyzed with a view to studying in any more detail the development of the *gel* structure as the system nears gelation. Examination of $P(Q)$ would seem to be a better way to study the evolving structure of the gel than study of the total scattering function $I(Q)$, since nothing particularly singular happens to $I(Q)$ at gelation, whereas, as has been discussed, $P(Q)$ may fall by orders of magnitude at small Q over a short time interval.

IV. CLUSTER ARRANGEMENT

To study the evolution of the arrangement of clusters in the DLCA system, we calculate the *cluster center-of-mass structure factor* $S_{CM}(\mathbf{Q},t)$. The center-of-mass coordinates $\mathbf{R}_j$ of the $N_c(t)$ clusters in the system at time t are inserted into Eq. (2) to give

$$S_{CM}(\mathbf{Q},t)=\frac{1}{N_c}\sum_{j}^{N_c}\sum_{k}^{N_c}\exp[i\mathbf{Q}\cdot(\mathbf{R}_j-\mathbf{R}_k)]. \qquad (10)$$

The center-of-mass vector of cluster j is given by

$$\mathbf{R}_j=\frac{1}{M_j}\sum_{k}^{M_j}\mathbf{r}_k, \qquad (11)$$

where the sum is over all the M_j particles in cluster j. $S_{CM}(Q)$, as the Fourier transform of the cluster position pair correlation function, describes the structure of cluster centers, or the arrangement of the clusters in the system. Plots of $S_{CM}(Q,t)$, circularly or spherically averaged as described above, are given in Fig. 6.

A. Evolution of $S_{CM}(Q)$

At very early time, $S_{CM}(Q)$ is approximately equivalent to $I(Q)$ since the system consists almost entirely of monomers (almost, because, as mentioned already, the random

TABLE II. Parameters of fits of the Fisher-Burford expression, (7) to cluster form factor data from three-dimensional simulations (see Fig. 3). ''Maximum Qd'' is the maximum value of Qd for which $P(Qd)$ data were used in the fit; d is the particle diameter. The accepted three-dimensional DLCA fractal dimension from mass-radius plots is $d_f \approx 1.75$ [12].

Density	Time	A	R_g	d_f	Maximum Qd
0.01	100	9.35	2.47	1.64	2.0
	200	25.20	4.16	1.85	1.5
	300	49.30	6.29	1.72	1.0
	500	102.60	8.32	2.19	0.8
0.05	5	3.62	1.43	1.33	2.0
	10	7.83	2.11	1.90	1.5
	20	22.87	3.72	2.04	1.6
	100	328.40	16.40	2.26	1.0
	100			1.63 [a]	
0.1	1	3.00	1.25	1.31	1.5
	3	8.33	2.16	1.97	1.5
	10	78.90	7.21	2.10	1.0
	20	941.20	28.20	2.03	1.0
	20			1.89 [a]	

[a]For the last times at the two higher densities, estimates of d_f from simple power-law fits to the $P(Qd)$ data, over the range $0.2 < Qd < 1.0$, are also given.

initial starting configuration on the lattice will contain some small clusters [17]). At Q greater than an upper limit Q_c, the center-of-mass structure factor is approximately constant at unity. Below Q_c, $S_{CM}(Q)$ decreases with decreasing Q, to some limit, at the smallest Q allowed by the system size Q_0, $S(Q_0)$. Analogously to the case of a simple hard-disk or hard-sphere system, the decrease of the cluster center-of-mass structure factor with decreasing Q below Q_c can be interpreted as a consequence of the ''confinement'' of the cluster centers by their immediate environment. As the aggregation proceeds the smallest-Q limit $S(Q_0)$ initially decreases with time so that the full S_{CM} curve between $Q = Q_0$ and $Q = Q_c$ steepens. That $S(Q_0)$ decreases in the early stages of the aggregation perhaps corresponds to the growth of space-filling structures (fractal clusters) that tends to increase the effective volume fraction of the system, resulting in a stronger confinement of cluster centers: Compare the case of an equilibrium hard-sphere or hard-disk fluid, where the structure factor at small Q decreases for increasing concentration. As the aggregation continues Q_c also decreases in time, indicating the growth of the typical intercluster length scale; cluster *centers* are getting further apart as the clusters grow (cluster surfaces, on the other hand, may still get closer together). Interestingly there is no strong *peak* in $S_{CM}(Q)$ near Q_c, as is seen in dense monodisperse hard-disk or hard-sphere systems [34]. The lack of a peak near Q_c indicates the lack of a very strongly preferred intercluster distance. Examination of pictures from the aggregation shows that there is a marked polydispersity in cluster sizes, as will be discussed below (also shown by more quantitative analysis of cluster size distributions [24]), which must also be involved in the wiping out of a strong peak in $S_{CM}(Q)$

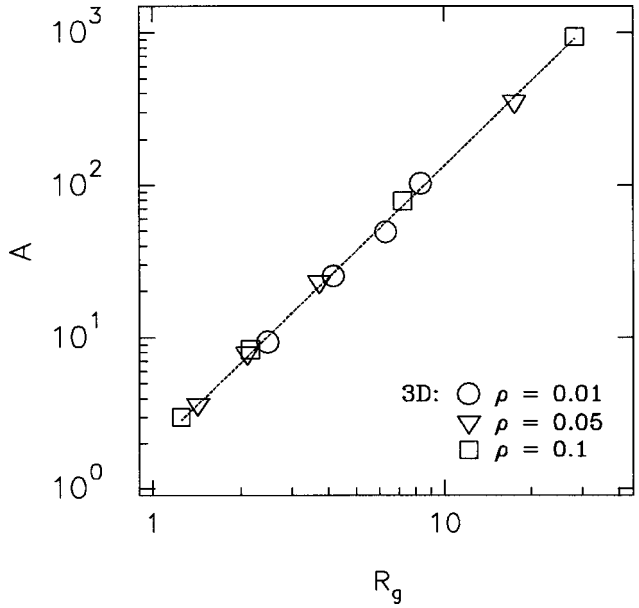

FIG. 4. Fisher-Burford fit amplitude parameter A vs radius parameter R_g (in particle diameters) [Eq. (7)], for Fisher-Burford fits to average form factor data from various example times during three-dimensional simulations. The line is a power-law fit to data from all number densities ρ; fitted exponents for this and for fits to each density separately are given in Table III.

TABLE III. Estimates of the average cluster fractal dimension d_f from Fisher-Burford fit parameters A and R_g for three-dimensional simulations.

Density	d_f
0.01	1.92
0.05	1.84
0.1	1.85
all	1.85

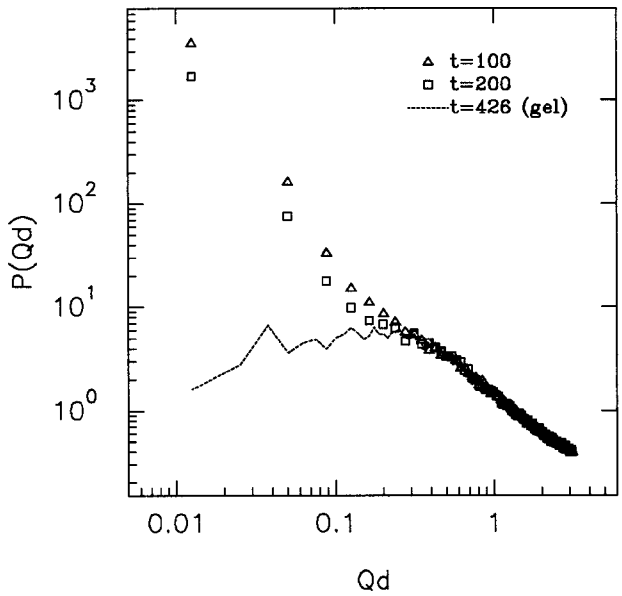

FIG. 5. Effect of gelation on the average form factor $P(Q)$. Data are from a two-dimensional simulation at number density $\rho = 0.3$.

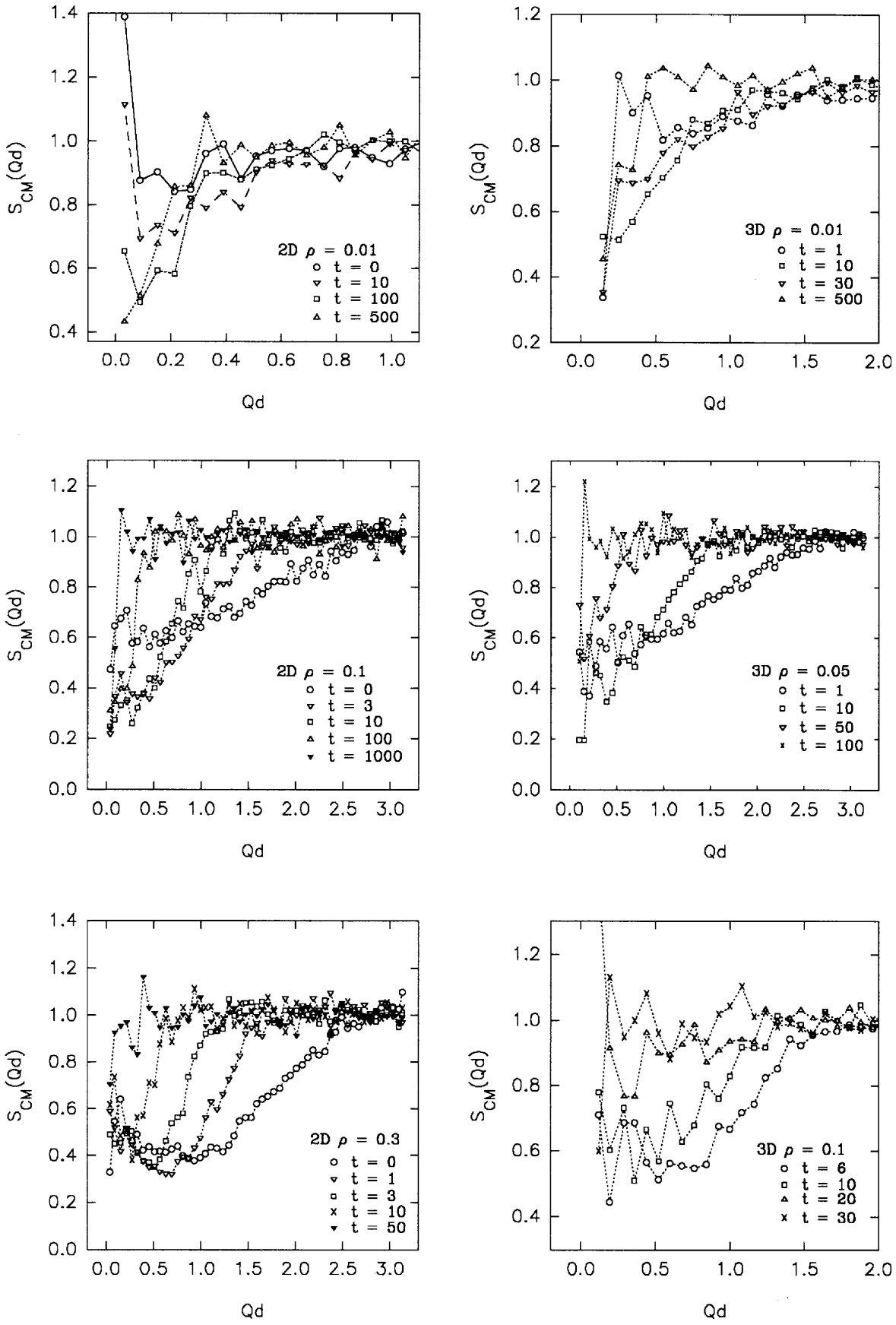

FIG. 6. Structure factors of the center-of-mass positions of clusters in DLCA simulations in 2D and 3D. The simulation system sizes are $L=500$ ($\rho=0.01$) (2D), $L=300$ ($\rho=0.1$ and 0.3) (2D), and $L=70$ (3D). The (dimensionless) x axis is Qd, where Q is the scattering vector magnitude in reciprocal particle diameters and d is the particle diameter.

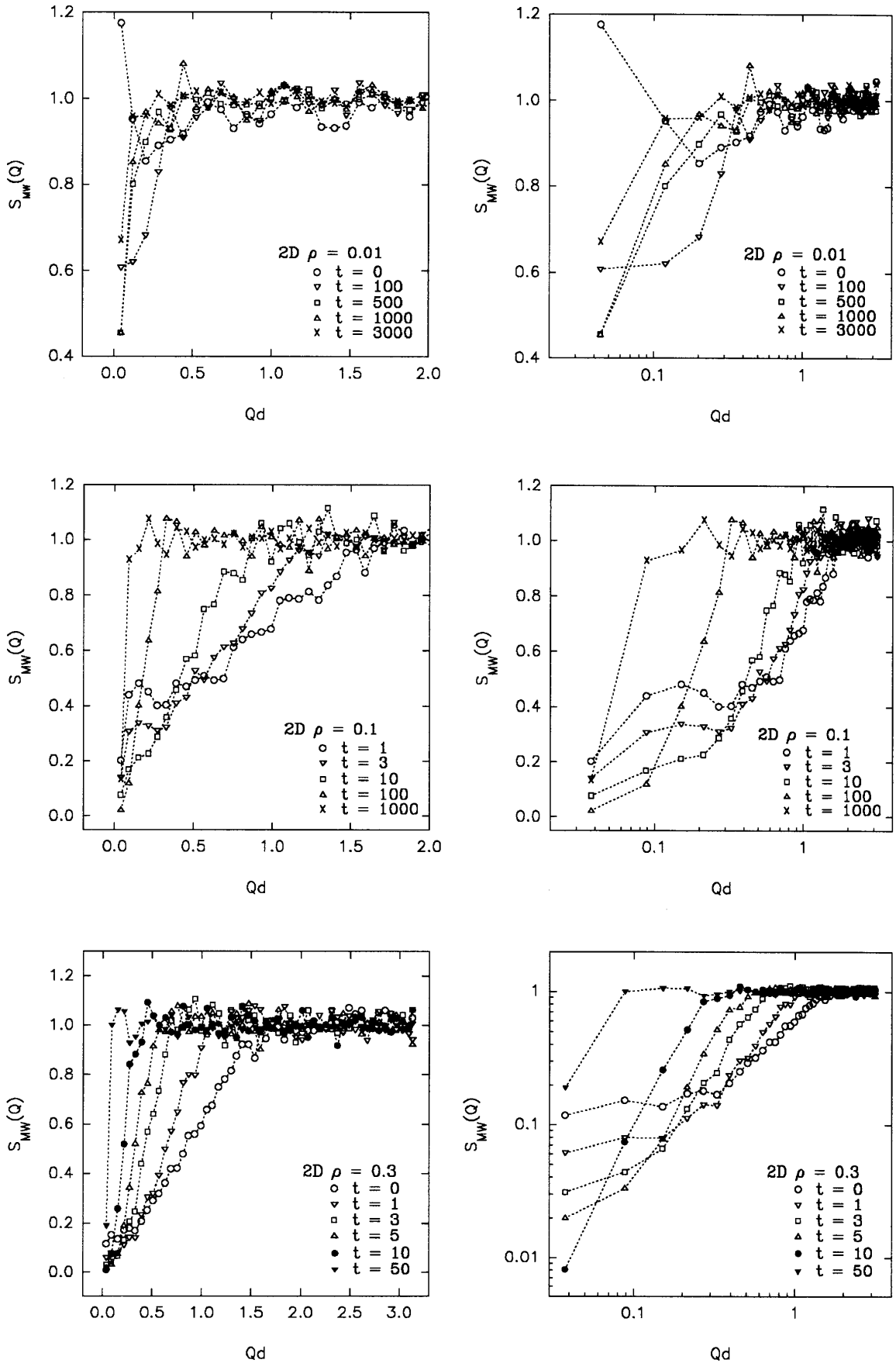

FIG. 7. Mass-weighted structure factors of the center-of-mass positions of clusters in DLCA simulations in 2D. Units are as in Fig. 6. $S_{MW}(Q,t)$ is calculated from Eq. (12). The right-hand column shows the same data in a log representation to more clearly demonstrate the behavior at small Qd.

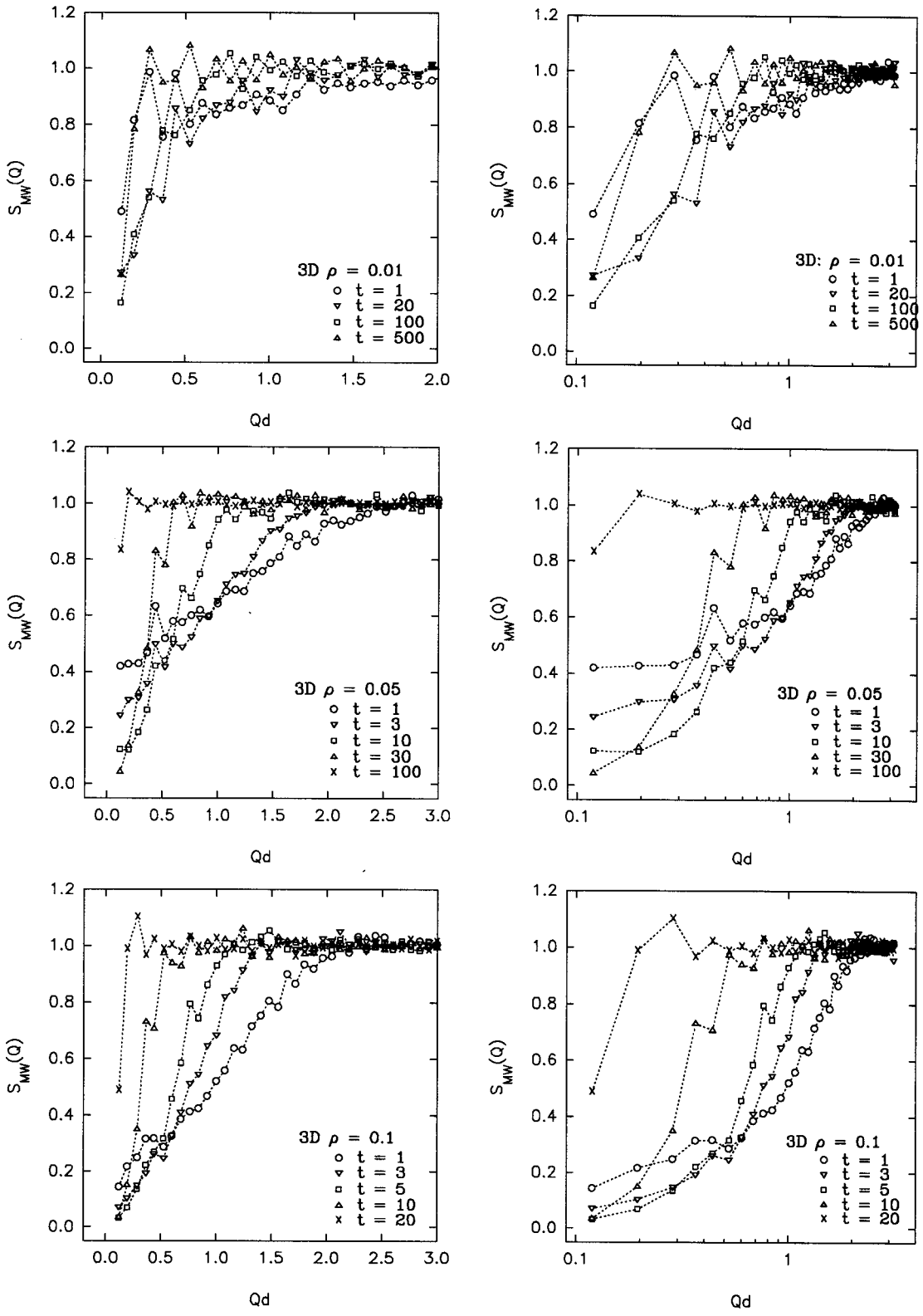

FIG. 8. Mass-weighted structure factors of the center-of-mass positions of clusters in DLCA simulations in 3D. Units are as in Fig. 6. The right-hand column shows the same data in a logarithmic representation to more clearly demonstrate the behavior at small Qd.

near Q_c [35]. Furthermore, one might expect the fractal clusters to be somewhat ''interpenetrable'' objects, which also would tend to imply the lack of a strongly preferred intercluster separation.

At the latest times Q_c approaches Q_0, that is, the intercluster length scale approaches the size of the system. $S(Q_0)$ begins to increase as fewer and fewer separate clusters occupy the system. Of course at the final point of the

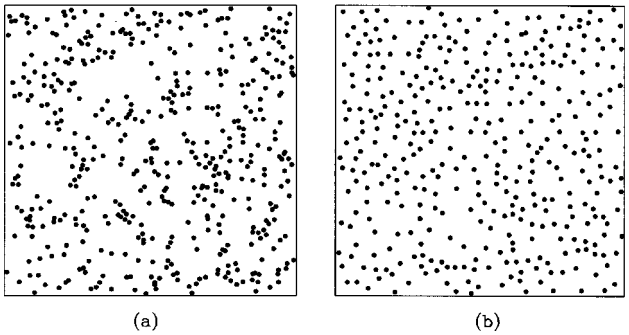

FIG. 9. Spatial distribution of the centers of clusters, in a two-dimensional DLCA simulation with system size $L=300$ and number density $\rho=0.3$, at time $t=10$: (a) clusters with mass $m<20$ and (b) clusters with mass $m\geqslant 20$.

simulation when all particles belong to a single cluster $S_{CM}(Q)$ trivially equals 1 at all Q: There is only one center of mass left in the system.

B. Size-position correlation

There is a clear rise in $S_{CM}(Q)$ at the smallest Q for the high-density systems (e.g., $\rho=0.3$ in 2D, Fig. 6). We can show by weighting the calculation of $S_{CM}(Q)$ that this rise is caused by the *smallest* clusters in the system. Figures 7 and 8 show the *mass-weighted cluster structure factor* $S_{MW}(Q)$ for the simulations, defined as

$$S_{MW}(\mathbf{Q})=\frac{1}{\sum_k M_k^2}\sum_j^{N_c}\sum_k^{N_c} M_j M_k \exp[i\mathbf{Q}\cdot(\mathbf{R}_j-\mathbf{R}_k)], \tag{12}$$

where again N_c is the number of clusters, M_k is the mass of cluster k, and $\mathbf{R}_k$ is the center of mass of cluster k. The normalizing factor is obtained by requiring that $S_{MW}(Q)$ approaches unity at large Q (where the ''self-terms'' $j=k$ dominate the sum in the numerator).

Such a mass-weighted structure factor has been employed before in studies of DLCA, e.g., Ref. [23]. We will consider its interpretation further in Sec. V; for now we use it simply to demonstrate the effect of cluster polydispersity on the arrangement of clusters in the DLCA system. The weighting in Eq. (12) reduces the contribution of *small* clusters to the cluster structure factor. The curve downward in the cluster structure factor between $Q\rightarrow 0$ and Q_c is noticeably steeper in $S_{MW}(Q)$, demonstrating that small clusters have significant effects on the center-of-mass structure even at very long length scales. Given that they are small clusters, this is at first rather surprising. The rise in the cluster structure factor at the smallest Q clearly observed in the highest-density systems is removed completely by the mass-weighting procedure. Such a rise in the structure factor at long length scales is indicative of long-length-scale inhomogeneities in the arrangement of the scatterers. In other words, the comparison of $S_{CM}(Q)$ and $S_{MW}(Q)$ indicates that the *smallest* clusters are not arranged homogeneously in the aggregating system. The arrangement of center-of-mass positions for ''small'' and ''large'' clusters is compared at one time step in a two-dimensional simulation at $\rho=0.3$ in Fig. 9. Here small clusters are those with mass less than 20 particles and large clusters have a mass of 20 or more particles. (For this time step the numbers of clusters in the two pictures are: 460 with $M<20$ and 370 with $M\geqslant 20$.) The inhomogeneity in the distribution of small clusters is striking when compared to the distribution of large clusters.

Such a *size-position correlation* is in fact familiar from general models of systems of *polydisperse* particles (see, e.g., [34]). Experimentally, Cabane *et al.* have discussed the importance of polydispersity in aggregation in the case of their siloxane polymer system [20]. While the DLCA system is often described as being composed of nearly monodisperse clusters (which makes theoretical approaches more straightforward), clearly the polydispersity of the clusters does have substantial effects on the long-length-scale structure of the system.

V. SEPARATION OF SCATTERING

A. $P(Q)$ and $S_{CM}(Q)$

In experimental scattering studies of colloidal suspensions the measured scattered intensity $I(Q)$ is often separated into two factors [34]: the *particle form factor* $P(Q)$ and the *structure factor* $S(Q)$

$$I(Q)=NP(Q)S(Q). \tag{13}$$

N is the total number of scatterers in the system. This factorization reflects the conceptual separation of two ''elements'' of structure in the suspension: $P(Q)$ describes the *internal structure* of the scatterer, and $S(Q)$ the *configuration* of the scatterers. Our calculated *cluster* form factors and cluster position structure factors can be seen as analogous quantities, if we consider our ''scatterer'' to be a *cluster*; our $S_{CM}(Q)$ then measures the configuration of the clusters. The question arises then whether the total scattering function in the DLCA simulations is in fact given by the product of the cluster form factor and the cluster center-of-mass structure factor, i.e., whether we can write

$$I(Q)\overset{?}{=}P(Q)S_{CM}(Q). \tag{14}$$

A key assumption involved in such a factorization is that the scatterers are *identical*, so that the form factor $P(Q)$ may be extracted as a multiplicative factor from the expression for $I(Q)$. While of course it is not true that the clusters in the DLCA system are identical, still, given that we orientationally average $P(\mathbf{Q})$ and average over many clusters to obtain $P(Q)$, the *average* cluster form factor may be sufficient to characterize the scattering behavior of the ''typical'' cluster, such that Eq. (14) is approximately satisfied.

In Figs. 10 and 11 we compare calculated scattering functions $I(Q)$ with the product $P(Q)S_{CM}(Q)$ at various times for example simulations in 2D and 3D. The results shown are typical of all times at all system densities studied. It is quite clear that Eq. (14) is not generally satisfied for the DLCA system. Only at large Q (short length scale) and then only at later times does the relation hold. At large Q we find that the cluster structure factor $S_{CM}(Q)\approx 1$ and $I(Q)\approx P(Q)$. Not surprisingly, the total scattering function at large Q or short

length scales is determined by the internal structure of clusters and does not depend on the arrangement of clusters. The averaging over clusters and over orientations means that detailed differences in the structure of different clusters are not observable in $P(Q)$ or in $I(Q)$ at large Q. The factorisation becomes better *at later times* at large Q probably because there are fewer small clusters and thus most of the scattering at the given length scale is by clusters that are larger than that scale. In that case any polydispersity in the sizes of these clusters will not strongly affect $P(Q)$ on this length scale. At small Q or long length scale, however, it is clear that the total scattering function cannot be separated simply into the two factors $P(Q)$ and $S_{CM}(Q)$.

B. Other approaches

A similar test of the separation of $I(Q)$ into factors separately describing the internal cluster structure and the cluster arrangement in two-dimensional DLCA simulations was briefly considered by Sciortino *et al.* in Ref. [23]. However, these authors used the mass-weighted structure factor $S_{MW}(Q)$ as defined in Eq. (12) to test the factorization:

$$I(Q) \stackrel{?}{=} P(Q)S_{MW}(Q). \tag{15}$$

They found that such a relation is satisfied, but only in systems at low number density. In fact, from our data we draw a similar conclusion, as some example plots show in Fig. 12. Over a limited time regime in the lower-density simulations (e.g. $\rho=0.1$ in 2D) $I(Q)\approx P(Q)S_{MW}(Q)$, while in the high-density simulations (e.g., $\rho=0.3$ in 2D) we never observe a time regime where the mass-weighted factorization works. Results are similar in both two- and three-dimensional simulations. Sciortino *et al.* do not consider further the physical significance of S_{MW}. Indeed its meaning is not clear: while S_{CM} can be reasonably clearly defined in terms of (the Fourier transform of) the cluster position pair correlation function, such a basic relation of S_{MW} to structure is not imme-

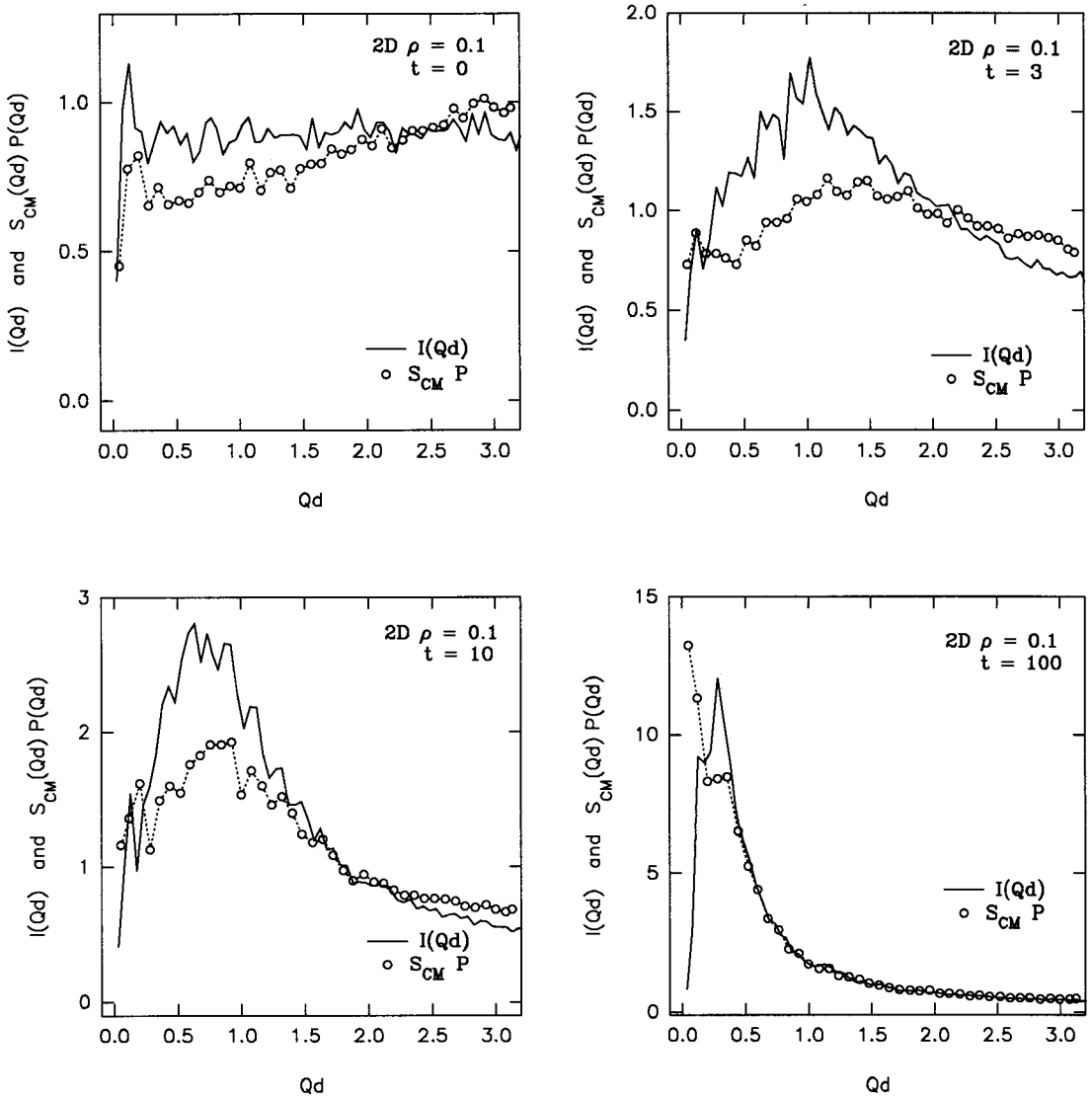

FIG. 10. Test of the ''separation'' of the total scattering function $I(Q)$ into average form factor $P(Q)$ and cluster center-of-mass structure factor $S_{CM}(Q)$. $I(Q)$, calculated from Eq. (2), is compared with the product $S_{CM}(Q)P(Q)$ for various times in a two-dimensional simulation at $\rho=0.1$, system size $L=300$.

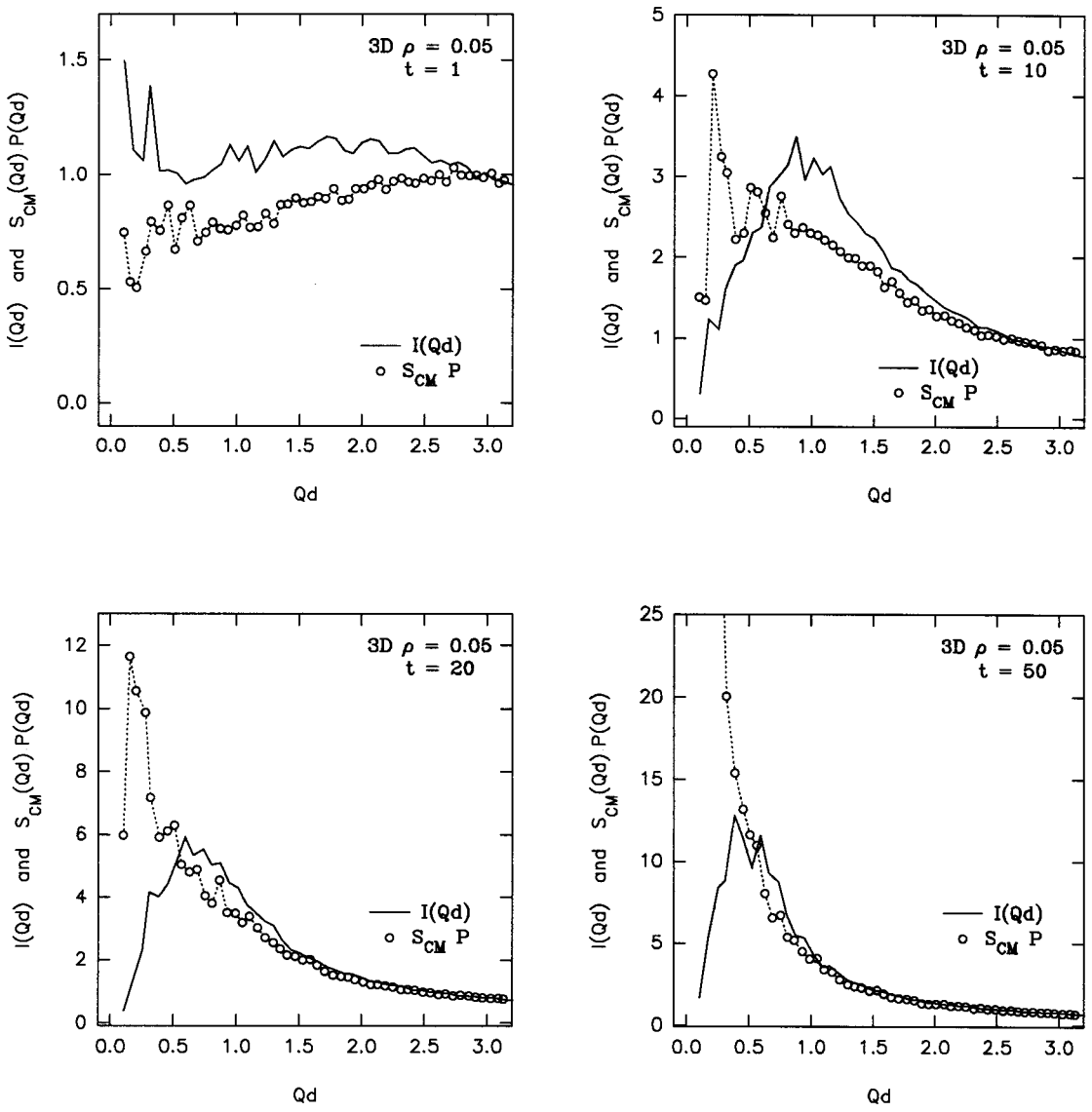

FIG. 11. Test of the separation of the scattering function $I(Q)$ into average form factor $P(Q)$ and cluster center-of-mass structure factor $S_{CM}(Q)$ for a three-dimensional simulation at $\rho=0.05$, system size $L=70$.

diately apparent. Effectively S_{MW} ''mixes'' the cluster arrangement with information on the *spatial mass distribution*. Of course, if all clusters have the same number of particles then S_{MW} is equal to S_{CM}. But if not, then S_{MW} does not so clearly describe the arrangement of the clusters.

Another way of looking at the mass weighting is that it simply allows the largest clusters to dominate the calculated structure factor. This might well be expected to improve the factorization of $I(Q)$ since it will reduce the importance of cluster polydispersity by strongly reducing the contribution of small clusters to the calculation. That the mass-weighted factorization fails in high-density systems is consistent with the observation that cluster size polydispersity increases very strongly as the system approaches gelation [24,33]; in high-density systems the effects of gelation are apparent very early on in the aggregation. Additionally, as we have shown, the arrangement of small clusters is not homogeneous, which may also have important effects on the factorization of $I(Q)$ into form factor and non-mass-weighted structure factor.

A different approach to the description of the scattering behavior of the aggregating system has been followed by Carpineti *et al.* in their examination of results from small-angle light-scattering experiments [7]. These authors define the ''scatterer'' in the aggregating system not simply as the fractal cluster but as the fractal cluster *plus its surrounding ''depletion zone.''* (The cluster plus depletion zone picture of the aggregating system has been studied via the pair correlation function $g(r)$ of the whole system in DLCA simulations [16–18].) The approach of Carpineti *et al.* seems promising given that the scattering by such an object does indeed fit the measured scattering data well, at least in low concentration systems at times sufficiently before gelation (at later times it is found necessary to fit the measurements using not simply the cluster plus depletion zone form factor but the product of the form factor and a calculated hard-sphere structure factor). Nevertheless, the direct physical definition of an individual cluster plus depletion zone object remains problematic [9]. As pointed out by Carpineti *et al.* in Ref. [7], the roles of the form factor and structure factor are not so well defined in a system of aggregating fractal objects (compared, for instance, to a suspension of monodisperse hard spheres). Even

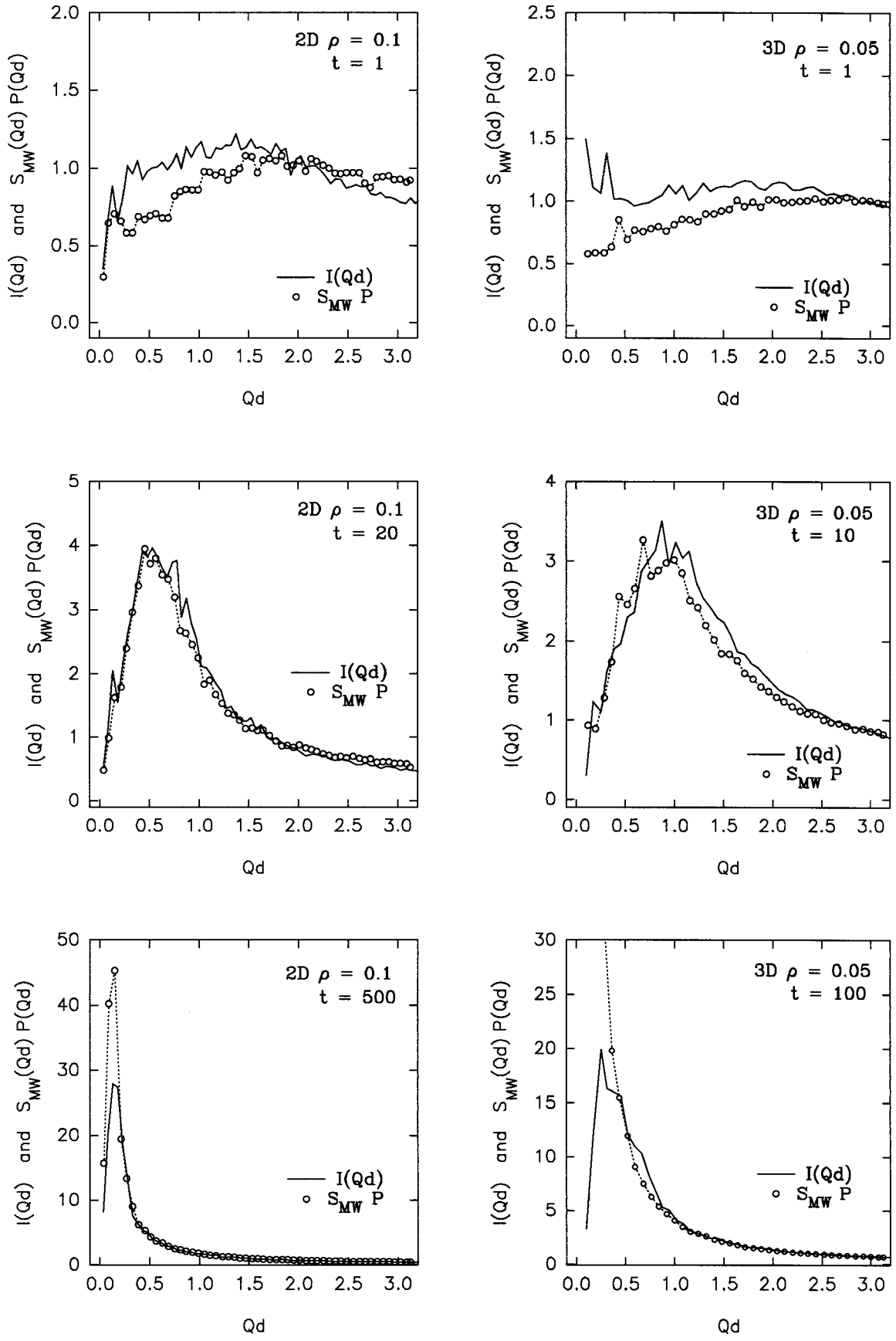

FIG. 12. Tests of the separation of the scattering function $I(Q)$ into average form factor $P(Q)$ and *mass-weighted* cluster center-of-mass structure factor $S_{MW}(Q)$ for DLCA simulations in 2D and 3D.

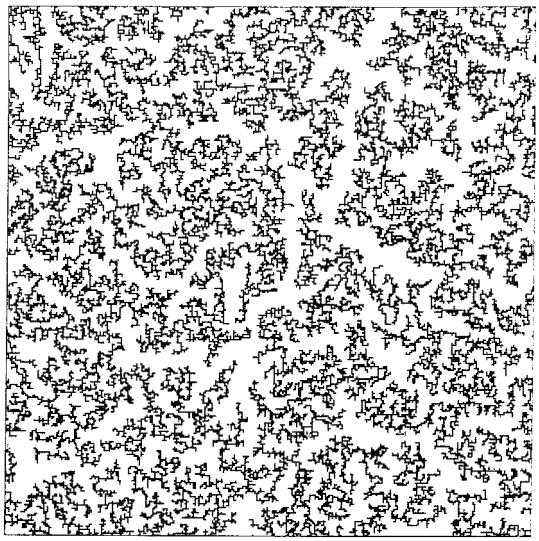

FIG. 13. Snapshot of the two-dimensional DLCA system with system size $L=300$ and number density $\rho=0.3$, at the final ''gel'' time when all particles belong to a single, connected, space-filling cluster. Neighboring surface shape correlations appear to generate channels through the structure.

so, especially in simulations it is quite simple to physically define the form factor, derived from the internal structure of the clusters, and the structure factor, derived from the arrangement of the clusters; this is indeed what we have done here. As we have shown, contrary to the case of a monodisperse suspension, in the aggregating system these two factors are not sufficient to completely describe the scattering behavior. In fact, they probably should not be called factors at all since they cannot be extracted as mathematical factors from the scattering function.

It remains the case that in the DLCA simulations the structure of clusters and the position of clusters are correlated if only in terms of the dependence between cluster size and cluster arrangement. That the factorization of the scattering function using the mass-weighted structure factor ''works'' at low density does not yet have a clear meaningful interpretation in terms of a correlation between the cluster structure and arrangement. In systems at high density (thus in *any* system close to gelation where the clusters fill space) there may be other elements of correlation between the structures of different clusters. For instance, snapshots of the simulation configurations at high number density (Fig. 13) are suggestive that the *surface structures* of neighboring clusters are strongly correlated. We hope to develop quantitative methods to study this possibility in future work.

VI. CONCLUSION

In this paper we have used methods analogous to scattering experiments to analyze in detail the structure of the DLCA simulation system, studying both the structure of individual clusters and the arrangement of these clusters in the system. In two-dimensional simulations, the *average cluster form factor* $P(Q)$ cannot be adequately fitted using the empirical Fisher-Burford form for a single, finite, circularly or spherically symmetric cluster. The reason for this is not clear. The effects on the average cluster form factor of cluster anisotropy and of the form of the cluster size distribution require further investigation. In three-dimensional simulations, $P(Q)$ is better fitted by the Fisher-Burford form, though again it seems the fit is not perfect. In particular, the fractal dimensions generated from the Fisher-Burford fits do not agree very well with those estimated from power-law fits nor with the accepted estimates from the fractal mass-radius relation. On the other hand, the mass and radius parameters from the three-dimensional Fisher-Burford fits are related according to the expected power law with an exponent agreeing reasonably well with the accepted DLCA fractal dimension. Experiments that directly measure $P(Q)$ in both two- and three-dimensional systems would be of great interest.

Near gelation, $P(Q)$ begins to decrease at the smallest Q (longest length scales): $P(Q)$ must approach the final total scattering function $I(Q)$ when the system contains only a single cluster and $I(Q)$ for the gel is peaked at $Q>0$. Successive measurements of the average form factor closer and closer to gelation in an experiment, by dilution, might represent a method of studying the time development of the space-filling gel structure at long length scales.

The cluster center-of-mass structure factor $S_{CM}(Q)$ may be used to study the arrangement of clusters in the system. $S_{CM}(Q)$ indicates that there is significant intercluster interaction in the DLCA system. Growing, near-impenetrable fractal clusters become increasingly confined by their neighbors. An important finding is that as the aggregation proceeds the arrangement of the surviving smallest clusters in the system becomes *inhomogeneous*, leading to noticeable effects in $S_{CM}(Q)$ at long length scales, particularly at high number density. This correlation between the size and arrangement of clusters is in fact expected for any system of polydisperse particles: The small particles can get into (or in this case are left behind in) the gaps between the large particles. The analysis presented here demonstrates that cluster polydispersity does have effects on the cluster arrangement, despite the common assumption in DLCA studies that the mass distribution is strongly peaked enough that the system can be taken as monodisperse. A complete description of the structure of the DLCA system must include these effects of polydispersity on cluster arrangement.

The separation of scattering into an average cluster form factor and a center-of-mass structure factor does not generally work for the DLCA system: $I(Q)\neq P(Q)S_{CM}(Q)$. This might be expected for various reasons. First, the DLCA system certainly does not consist of identical clusters, though averaging over a distribution of clusters and over orientations ought to reduce the importance of this polydispersity. However, the size-position correlation discussed above also will lead to the breakdown of the separation of scattering. The scattering by a particular cluster (which depends on cluster size, cluster shape, etc.) is correlated with the cluster's position, thus the single-particle scattering factors and the cross-particle interference factors are not independent and $P(Q)$ cannot be factorized out of the expression for the total scattering. However, as also demonstrated by other authors [23], a factorization of the scattering function into average form factor and *mass-weighted* structure factor S_{MW} is possible in low-density systems far from gelation. This is possibly due at least in part to the dominance of large clus-

ters in the S_{MW} function, which tends to reduce the importance of cluster polydispersity. In any case, the physical interpretation of S_{MW} is not so straightforward. S_{CM} directly describes the arrangement of clusters. S_{MW}, on the other hand, mixes cluster arrangement with cluster size. Further work on the meaning of S_{MW} and more generally on the nature of cross correlations between different clusters in the DLCA system is clearly required.

ACKNOWLEDGMENTS

We acknowledge useful discussions over the course of this work with J. C. Earnshaw and A. D. Bruce and development work on simulation algorithms by M. Sievwright. The work was partly supported by the U.K. Engineering and Physical Sciences Research Council. The simulations were performed on an Alpha AXP workstation, kindly provided by Digital Equipment Corporation.

[1] M. Carpineti and M. Giglio, Phys. Rev. Lett. **68**, 3327 (1992).
[2] J. Bibette, T. G. Mason, H. Gang, and D. A. Weitz, Phys. Rev. Lett. **69**, 981 (1992).
[3] D. J. Robinson and J. C. Earnshaw, Phys. Rev. A **46**, 2045 (1992); **46**, 2055 (1992); **46**, 2065 (1992).
[4] M. Carpineti and M. Giglio, Phys. Rev. Lett. **70**, 3828 (1993).
[5] D. J. Robinson and J. C. Earnshaw, Phys. Rev. Lett. **71**, 715 (1993).
[6] J. Bibette, T. G. Mason, H. Gang, D. A. Weitz, and P. Poulin, Langmuir **9**, 3352 (1993).
[7] M. Carpineti, M. Giglio, and V. DeGiorgio, Phys. Rev. E **51**, 590 (1995).
[8] W. C. K. Poon, A. D. Pirie, and P. N. Pusey, Faraday Disc. **101**, 65 (1995).
[9] W. C. K. Poon and M. D. Haw, Adv. Colloid Interface Sci. (to be published).
[10] P. Meakin, Phys. Rev. Lett. **51**, 1119 (1983).
[11] M. Kolb, R. Botet, and R. Jullien, Phys. Rev. Lett. **51**, 1123 (1983).
[12] R. Jullien, M. Kolb, and R. Botet, J. Phys. (France) **45**, L211 (1984).
[13] M. D. Haw, W. C. K. Poon, and P. N. Pusey, Physica A **208**, 8 (1994).
[14] A. Hasmy, E. Anglaret, M. Foret, J. Pelous, and R. Jullien, Phys. Rev. B **50**, 6006 (1994).
[15] T. Sintes, R. Toral, and A. Chakrabarti, Phys. Rev. E **50**, R3330 (1994).
[16] A. E. Gonzalez and G. Ramirez Santiago, Phys. Rev. Lett. **74**, 1238 (1995).
[17] M. D. Haw, M. Sievwright, W. C. K. Poon, and P. N. Pusey, Physica A **217**, 231 (1995).
[18] A. Hasmy and R. Jullien, J. Non-Cryst. Solids **186**, 342 (1995).
[19] A. E. Gonzalez and G. Ramirez Santiago, J. Coll. Int. Sci. **182**, 254 (1996).
[20] B. Cabane, M. Dubois, and R. Duplessix, J. Phys. (France) **48**, 2131 (1987).
[21] M. Dubois and B. Cabane, Macromolecules **22**, 2526 (1989).
[22] M. Kallala, C. Sanchez, and B. Cabane, Phys. Rev. E **48**, 3692 (1993).
[23] F. Sciortino and P. Tartaglia, Phys. Rev. Lett. **74**, 282 (1994); F. Sciortino, A. Belloni, and P. Tartaglia, Phys. Rev. E **52**, 4068 (1995).
[24] M. D. Haw, Ph.D. thesis, University of Edinburgh, 1996 (unpublished).
[25] W. H. Press, S. A. Teukolsky, W. T. Vetterling and B. P. Flannery, *Numerical Recipes* (Cambridge University Press, Cambridge, 1993), Chap. 12.
[26] See, for example, D. Stauffer, A. Coniglio, and M. Adam, Adv. Polym. Sci. **44**, 103 (1982); J. Bauer, N. Dingenouts, and M. Ballauff, Acta Polym. **45**, 430 (1994); V. Trappe, J. Bauer, M. Weissmueller, and W. Burchard, Macromolecules **30**, 2365 (1997).
[27] M. Carpineti, F. Ferri, M. Giglio, E. Paganini, and U. Perini, Phys. Rev. A **42**, 7347 (1990).
[28] J. E. Martin and A. J. Hurd, J. Appl. Crystallogr. **20**, 61 (1987).
[29] M. E. Fisher and R. J. Burford, Phys. Rev. **156**, 583 (1967).
[30] R. Thouy and R. Jullien, J. Phys. (France) I **6**, 1365 (1996).
[31] M. Kolb and H. J. Herrmann, J. Phys. A **18**, L435 (1985).
[32] A. J. Armstrong, R. C. Mocklet, and W. J. O'Sullivan, J. Phys. A **19**, L123 (1986).
[33] J. C. Gimel, D. Durand, and T. Nicolai, Phys. Rev. B **51**, 11 348 (1995).
[34] P. N. Pusey, in *Liquids, Freezing, and the Glass Transition*, edited by J. P. Hansen, D. Levesque, and J. Zinn-Justin (Elsevier, Amsterdam, 1991).
[35] P. van Buerten and A. Vrij, J. Chem. Phys. **74**, 2744 (1981).